Operating Parameters of a Quadrupole in a Grounded Cylindrical Housing*

D. R. Denison

University Instruments Corporation, Boulder, Colorado 80301

Quadrupole theory and design are based on the solution of Mathieu's equations, which assume that zero potential, except for the symmetry axes between the electrodes, is infinitely far away. In practice, the quadrupole rods are mounted within a grounded housing not much larger than the electrode structure itself. This study determines the operating parameters and optimum electrode size for a quadrupole with electrodes of circular cross section located within a zero-potential cylindrical surface. It is found that the rod size is only weakly dependent on the location of the external, zero-potential surface and the optimum rod size is $r=1.1468r_0$ for a cylinder radius of $3.54r_0$. Although the optimum rod size is only 1.15% smaller than the commonly used value of $r=1.16r_0$, it is found that 43% higher sensitivity at a resolution of 400 (ΔM measured at half-height) results from using the optimum radius electrodes.

Introduction

The quadrupole mass analyzer, first described by Paul and Steinwedel[1] in 1953, and subsequently discussed by many authors, consists ideally of hyperbolic electrodes of infinite extent with zero-potential lines existing along the asymptotes of the hyperbolas. When the possibility of replacing the hyperbolic electrodes by electrodes of circular cross section was presented by Dayton *et al.*[2] while studying the magnetic quadrupole, zero potential (magnetostatic) existed along the lines equidistant from pairs of electrodes and at infinite distance from the electrode structure. This technique was adopted by Paul, Reinhard, and von Zahn[3] for the electrostatic quadrupole and zero potential was treated as being infinitely far from the quadrupole (except for the symmetry axes). In reality, the quadrupole structure is operated within a vacuum chamber which is normally metallic and at ground potential. This paper presents data on the operating parameters of a quadrupole with circular cross-section electrodes in a grounded cylindrical housing. Dayton empirically determined the optimum radius of the circular electrodes to be $r=1.148r_0$, where $2r_0$ is the spacing between diametrically opposite electrodes. Curiously, the paper by Paul, Reinhard, and von Zahn[3] misquoted Dayton by using $r=1.16r_0$. Even more curious, later authors have used the misquote while referencing the work of Dayton.

* Some of the computer techniques used in this study were developed while the author was at Granville–Phillips Co.

Optimization of Electrode Size

The potential distribution in a quadrupole with circular crossection electrodes cannot be explicitly written, but can be expressed as an infinite series.

$$\phi=(U+V\cos\omega t)\sum C_m(r/r_0)^m\cos m\theta, \qquad (1)$$

which is a multipole expansion and is a solution to Laplace's equation

$$\nabla^2\phi=0. \qquad (2)$$

Here U is the applied dc voltage and $V\cos\omega t$ is the applied rf voltage. The symmetry of the potential requires that the potential change sign when θ changes by $\pi/2$. Thus

$$\cos m\pi/2=-1, \qquad (3)$$

which implies $m=2, 6, 10, 14, \cdots$, or

$$\phi=(U+V\cos\omega t)\sum_{n=0}^{\infty} C_n\left(\frac{r}{r_0}\right)^{2(2n+1)}\cos[2(2n+1)\theta]. \qquad (4)$$

The first term is the quadrupole term, the second is a 12-pole term, the third is a 20-pole term, etc. The 12-pole term is the next largest term in most of the central region and thus the best approximation to a pure quadrupole potential is an electrode radius such that $C_1=0$. The technique of determining the values of the coefficients, C_n, as a function of electrode radius is as follows:

(1) The Liebmann technique[4] is used with a digital computer to compute numerically the potential dis-

tribution at a large number of equally spaced points within the electrode structure. Figure 1 shows a series of equipotentials for one quadrant of the electrode structure.

(2) For values of the potential at these points within a circle of radius r_0 centered within the quadrupole structure, the radius r and angle θ of each point are used to obtain simultaneous equations for the C_n.

(3) A finite number of C's are evaluated by a least-squares fit of Eq. (4) to the data points. The number of C's evaluated was increased until no change was observed in the first five coefficients. This occurred with 12 terms. Thus, 12 coefficients were obtained by a least-squares fit to about 250 points. Figure 2 gives C_1 as a function of r/r_0 for two cases: ground at infinity and ground at $R=3.54r_0$ (the smallest practical cylinder radius). As the zero-potential surface decreases in radius, the optimum electrode radius increases. In the case of the round-rod quadrupole, the change in rod radius is very small except for large r_0 instruments.

Equation (4) can be differentiated to give the equations of motion which can be numerically integrated to give ion trajectories. A number of interesting points come to light when this is done. The equations of motion can be written in rectangular coordinates:

$$d^2x/d\tau^2 = -(a+q\cos\tau)\sum C_n \frac{2n+1}{4}\left(\frac{x^2+y^2}{r_0}\right)^{2n} \times\{x\cos[2(2n+1)\theta]+y\sin[2(2n+1)\theta]\}, \quad (5)$$

$$d^2y/d\tau^2 = -(a+q\cos\tau)\sum C_n \frac{2n+1}{4}\left(\frac{x^2+y^2}{r_0}\right)^{2n} \times\{y\cos[2(2n+1)\theta]-x\sin[2(2n+1)\theta]\}, \quad (6)$$

where $a=8eU/m\omega^2r_0^2$, $q=4eV/m\omega^2r_0^2$, $\tau=\omega t$, and $\theta=\tan^{-1}(y/x)$, as in the usual quadrupole parametric notation. It is a simple exercise to show that the quadrupole term ($n=0$) for each equation is dependent on a single coordinate rather than both x and y. However, higher multipole terms are x and y dependent. Thus, in a quadrupole structure with circular electrodes, the components of the ion motion in the x and y directions are not completely independent but are weakly coupled through the nonquadrupole field components.

As in the case of the pure quadrupole, these equations of motion result in bounded ion trajectories for only certain values of a and q. The a and q parameters for stable orbits can be obtained by numerical integration, and one obtains the corresponding stability diagram. The stability diagram obtained is similar to the a–q diagram for the hyperbolic electrode quadrupole in the geometric sense; i.e., the two stability diagrams, when normalized, are identical point

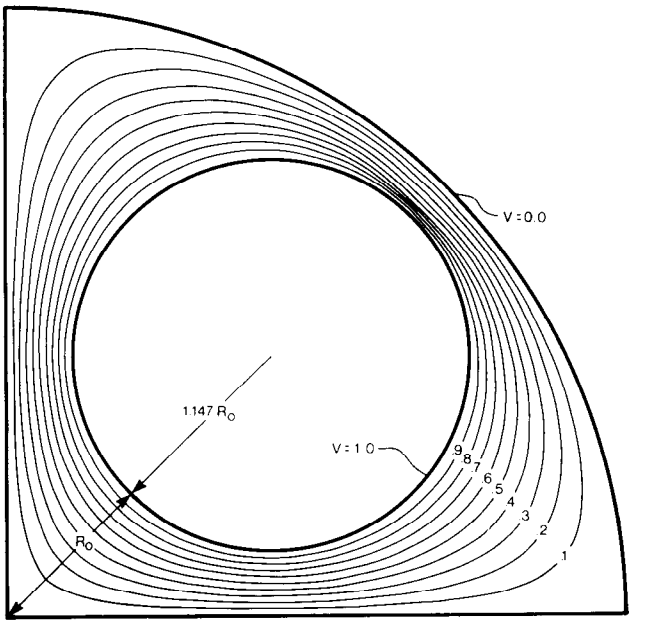

FIGURE 1. One quadrant of the potential distribution in a quadrupole with circular cross-section electrodes within a cylinder at zero potential.

for point. As can be seen in Fig. 3, the stability diagram for the circular electrode quadrupole is displaced toward higher values of a and q. The particular diagram shown is for a structure as Fig. 1 with the grounded surface at $R=3.54r_0$ and $r=1.1468r_0$, which gives $C_1=0$. For comparison, the stability diagram of a $r=1.16r_0$ structure is shown. The location of the stability diagrams shows the $r=1.1468r_0$ structure to be a better approximation to the pure quadrupole.

Effect of Operating Parameters

The change in electrode radius from $1.16r_0$ to $1.1468r_0$ is only 1.15%, but what is the effect on the

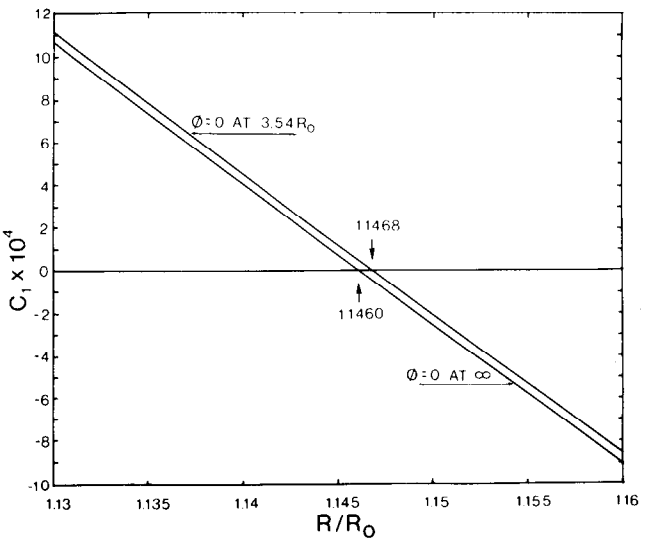

FIGURE 2. Variation of the coefficient of the 12-pole potential term with electrode radius.

quadrupole performance? Brubaker[5] showed that a "critical radius" exists beyond which an ion could not penetrate without colliding with an electrode, and the usable field radius in a quadrupole with $1.16r_0$ radius electrode is only 82% of the geometric radius r_0 at a resolution of 100. Thus, the circular electrode quadrupole had only 67% of the available crossection of a hyperbolic electrode quadrupole with the same r_0. At a resolution of 400 the available cross section has decreased to only 45% of the hyperbolic structure. Figure 4 shows the envelope of y motion for input conditions that result in unstable trajectories at resolutions of 100 and 400 in a $r=1.1468r_0$ circular electrode structure. The instability boundary occurs at $0.86r_0$ and $0.80r_0$, respectively. Thus, at a resolution of 100 the available cross section has increased by 10.0% and at a resolution of 400, the available cross section has increased by 42.6% over that of a structure with $r=1.16r_0$. The important thing here is that the effective cross section of the analyzer decreases less rapidly for the 1.1468-r_0 instrument than for the 1.16-r_0 device as the resolution is increased. It would appear then that in a given instrument with fixed entrance conditions for injecting the ions into the analyzer, the sensitivity of the 1.1468-r_0 rod analyzer should be less dependent on increasing resolution than the commonly used 1.16-r_0 rod analyzer.

The effect of the change in electrode size on voltage requirement is seen from the stability diagrams to be less than 1% and is, therefore, of little practical concern. A given mass appears at a different voltage than predicted by the stability diagram of the hyperbolic electrode quadrupole but the difference is small and rarely is the applied voltage used as a peak identification criterion.

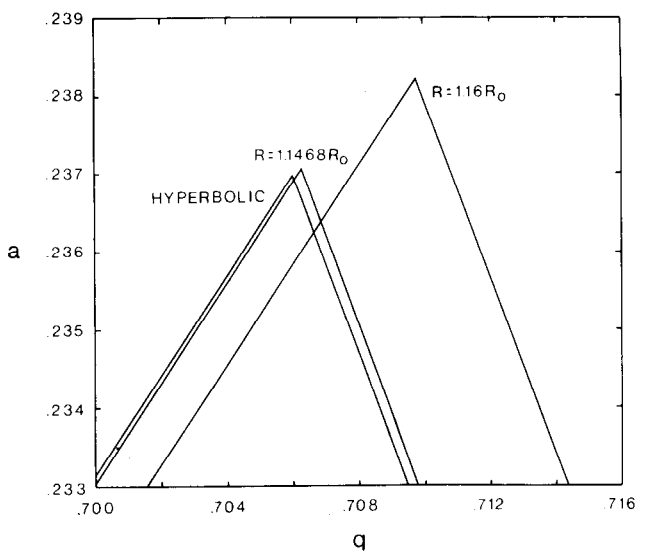

FIGURE 3. Location of the tips of the stability diagrams of a hyperbolic electrode quadrupole and circular electrode quadrupoles with rod radii of $1.1468r_0$ and $1.16r_0$.

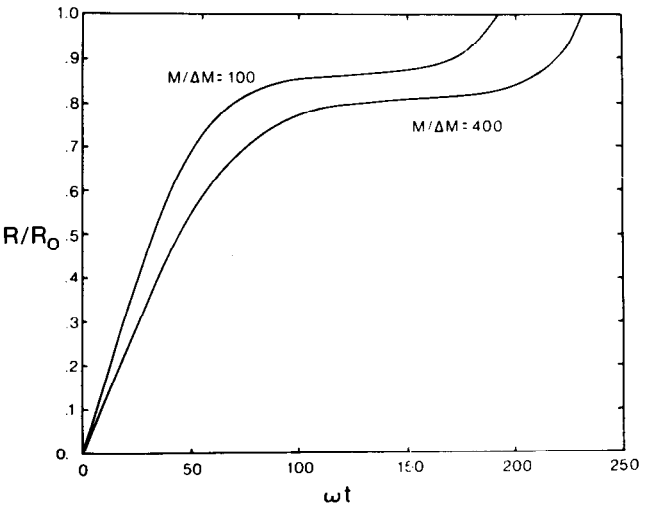

FIGURE 4. Envelopes of y-component motion of an ion in the field of a quadrupole with circular cross-section electrodes showing the "critical radius" for resolutions of 100 and 400. The radius of the electrodes is $r=1.1468r_0$.

Although the improvement in sensitivity is marked, there is no practical improvement in resolution. In practice, the resolution is limited by mechanical construction or electronic-circuit limitations to values lower than the theoretically achievable values even for $r=1.16r_0$. However, Dawson and Whetten[5] have shown theoretically that the sixth-order component to the potential (12 pole) can result in a blunted tip on the stability diagram and hence constitutes a limitation to the theoretically achievable resolution. The elimination of the sixth-order component thus may result in some theoretically improved resolution, but this requires further study.

From a practical point of view, the consequences of rod-radius optimization are even more pronounced. Paul *et al.*[3] showed that the power necessary to drive a hyperbolic electrode quadrupole is

$$W=6.5\times10^{-4}CM^2f^5r_0^4/Q, \qquad (7)$$

where C is the quadrupole capacitance in pf, M is the ion mass, f is the radio frequency in MHz, and Q is the circuit quality factor. The relationship, except for the constant, is the same for round-rod quadrupoles. For a resolution of 400 and the same sensitivity, a quadrupole with $1.1468r_0$ rods would have 83.75% of the electrode spacing of a $1.16r_0$ rod quadrupole. Thus, the power necessary to drive the $1.1468r_0$ rod radius quadrupole is less than half that necessary to drive the $1.16r_0$ rod radius instrument with the same sensitivity at a resolution of 400. This difference increases with increasing resolution.

Conclusion

It is found from the computer study that the assumption that zero potential is infinitely far from a quadrupole structure with circular electrodes is not

seriously in error. This probably results from the fact that the electrode radius for optimum fit to a quadrupole field is sufficiently large that the central region, where mass separation takes place, is not strongly influenced by external zero potential. The result might be different if the quadrupole were located in a high potential region with its center at zero potential, but this is not a common occurrence.

The sensitivity of a quadrupole with circular cross-section electrodes is strongly dependent on the ratio of electrode radius to electrode spacing. The current use of $r=1.16r_0$ for rod radius appears to penalize unnecessarily the performance of the circular electrode quadrupole. A better value for the rod radius would be a $1.147r_0$, which yields either higher sensitivity or a lower driving-power requirement.

References

1. W. Paul and H. Steinwedel, Z. Naturforsch. **A8**, 448 (1953).
2. I. E. Dayton, F. C. Shoemaker, and R. F. Mozley, Rev. Sci. Instrum. **25**, 485 (1954).
3. W. Paul, H. P. Reinhard, and U. von Zahn, Z. Physik **152**, 143 (1958).
4. See, e.g., K. S. Kunz, *Numerical Analysis* (McGraw-Hill, New York, 1957), p. 296.
5. P. H. Dawson and N. R. Whetten, J. Vac. Sci. Technol. **7**, 440 (1970).

Improved Method of the Resolution for Quadrupole Mass Spectrometers

T. Sakai, Y. Ino, and M. Sakimura

Vacuum Equipments Division, Nippon Electric Varian, Ltd., Fuchu, Tokyo, Japan

Resolution mode of quadrupole mass filter is well represented by mass scan line on stability diagram. All mass peaks just disappear on the cutoff scan line which passes through the origin and to the apex of the stability diagram. When a scan line is shifted downward by a small amount parallel to the cutoff scan line, it can be expected theoretically that all mass peaks give a constant peak width independent of mass. Adjustment of resolution is carried out based on this theory. As the peak height is proportional to the peak width, a mass spectrum obtained experimentally with this mode of operation gives a constant pattern coefficient in adjusting the resolution.